

Crystallite Size Effects in Chemisorption on Dispersed Metals

DINA FARIN AND DAVID AVNIR

*Department of Organic Chemistry and the Fritz Haber Research Center for Molecular Dynamics,
The Hebrew University of Jerusalem, Jerusalem 91904, Israel*

Received April 27, 1989

In the elucidation of the crystallite size, $2R$, of metals dispersed on inert supports, an assumption is made that $n_p \propto R^2$, where n_p is the chemisorption capacity of one particle. We have found that in many chemisorption studies the relation between n_p and R is more accurately given by $n_p \propto R^{D_c}$, $\sim 1.8 < D_c < \sim 2.2$. It is shown that some basic models of area-size relations can account for such D_c deviations from 2. These include small-size effects, size-dependent chemisorption stoichiometry, and the size-dependent ratio of the crystallographic planes. © 1989 Academic Press, Inc.

1. BACKGROUND

In this report we draw attention to a relatively small but significant effect (up to a factor of 2) regarding the calculation of particle size of dispersed metal catalysts from chemisorption data. We show that the common assumption

$$n_p = kR_c^2, \quad (1)$$

where n_p is the chemisorption of a single crystallite, $2R_c$ is its calculated size, and k , here and in all equations below, is a constant (obviously with various units), is in many instances inaccurate. We also show that based on elementary considerations of chemisorption on crystallites, Eq. (1) should be replaced by

$$n_p = kR^{D_c}, \quad (2)$$

where $2R$ is the independently determined size and most of the D_c (defined below) values cluster in the range ~ 1.8 – ~ 2.2 . It is shown in Section 2 that a large volume of chemisorption data obeys Eq. (2). In offering an explanation for this phenomenon, we shall not resort to causes such as $D_c \neq 2$ reflects systematic experimental errors; that $D_c > 2$ reflects (fractal) surface roughness (1); or that $D_c < 2$ reflects a (fractal) sub-set of active sites (2). Our aim is to show that D_c is expected to be different

from 2 prior to any considerations of that sort, and that the most basic considerations of the details of chemisorptions and crystallite structures indeed lead to empirical $D_c \neq 2$ situations. In particular, we show that the effects of the mere small size of the crystallites, the effects of various chemisorption stoichiometries, and the effects of varying proportions of crystallite low Miller index planes all create $D_c \neq 2$ situations.

We refer to D_c as the "chemisorption dimension" (not necessarily fractal) in order to comply with the many reported cases in which particle size effects on physisorption (1, 3), chemisorption (2, 4), and catalytic (5, 6) and noncatalytic (7, 8) interactions were found to be describable in terms of a power law, similar to Eq. (2), with a characteristic D (subscript denoting the process) value. All fall under the same practically useful umbrella of elucidating structural information by performing a resolution analysis (in our case with R as a yardstick). In many instances such analyses lead to a characteristic D value, from which information on the effective morphology, fractal or non-fractal, is obtained (9).

2. THE SET OF EQUATIONS EMPLOYED FOR THE ANALYSIS OF CHEMISORPTION DATA

The reanalysis of studies of chemisorption data on dispersed metals (Section 3)

was performed basically according to Eq. (2). Practically, however, we applied the following modifications of Eq. (2), tailored to the ways the chemisorption data are reported:

(a) Quite often, the chemisorption capacity is given in terms of the metal surface area, A_{av} (m^2/g metal). This is calculated from averaged constants (10) as

$$A_{av} = N_0 \cdot n_m \cdot n_s^{-1} \cdot X_m, \quad (3)$$

where N_0 is Avogadro's number, n_m is the chemisorption capacity (moles/g), n_s is the number of metal atoms per unit area (atoms/ m^2 , for which an average of the main low index planes is taken), and X_m is the chemisorption stoichiometry (i.e., the average number of surface metal atoms associated with the adsorption of one molecule.)

(b) In many other instances the chemisorption data are reported directly in terms of the particle size derived from A_{av} . The procedure (11) is to use the specific volume of the metal, V_{sp} (volume/g), in order to estimate the thickness or size, $2R_c$, from

$$V_{sp} = 2 \cdot f \cdot A_{av} \cdot R_c, \quad (4)$$

where f is the shape factor for the packing of the metal. Since V_{sp} and f are constants, Eq. (4) can be rewritten as

$$R_c = kA_{av}^{-1}. \quad (5)$$

(c) Another common way to express the surface area is through the "dispersion" of the metal. The two are related through (12)

$$\text{dispersion} = w_a \cdot A_{av} \cdot N_0^{-1} \cdot n_s, \quad (6)$$

where w_a is the atomic weight of the metal.

In order to apply these types of data for the evaluation of D_c we first convert Eq. (2) to units of mole/g. Since, for compact crystallites which are not mass-fractals, the number of crystallites per g depends linearly on R^{-3} (13), one obtains

$$n_m = kR^{D_c-3}. \quad (7)$$

And since the measurable quantity, n_m , is related to the reported value of A_{av} through

constants (Eq. (3)), one arrives at the relation

$$A_{av} = kR^{D_c-3}. \quad (8)$$

It is important to mention here that since n_s and X_m (in Eq. (3)) can change with size (see Section 4), the true surface area $A(R)$ depends on R in a more complex way, through an R -dependent k :

$$A(R) = k(R)R^{D_c-3}. \quad (9)$$

One is advised therefore to use either n_m directly (Eq. (7)) or a direct representation of it (Eq. (8)).

Similarly, since R_c is related to A_{av} through a constant (Eq. 5)), one can use reported values of R_c as follows (from Eq. 8)):

$$R_c = kR^{3-D_c}. \quad (10)$$

Equation (10) is an important result. It emphasizes that a priori one cannot make the assumption $R_c = R$; it holds only for $D_c = 2$ and $k = 1$.

Also, since the dispersion is related to A_{av} through constants (Eq. (6)), one gets

$$\text{dispersion} = kR^{D_c-3}. \quad (11)$$

In summary, Eqs. (8), (10), and (11) allow the use of reported chemisorption data for the evaluation of D_c .

When this type of conversion of equations is carried out on a single-particle level, different relations are obtained. For instance, from Eqs. (1) and (2) one obtains directly the single-particle analog of Eq. (10),

$$R_c = kR^{D_c/2}. \quad (12)$$

Notice that Eqs. (10) and (12) are seemingly contradictory. This is explained in Section 5.

3. THE RESULTS OF THE REANALYSIS OF CHEMISORPTION DATA

The reanalysis of a large volume of chemisorption data showed that this process is describable in terms of the more general Eq. (2) (rather than Eq. (1)), or in terms of

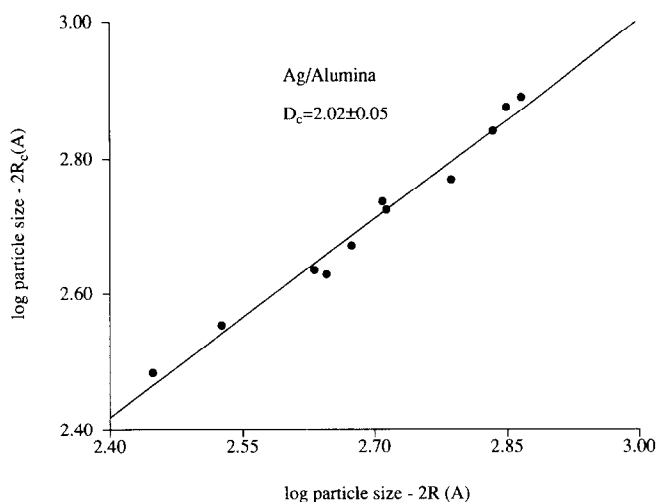


FIG. 1. Ag crystallite size, $2R_c$ (Å), measured by O_2 chemisorption as a function of Ag crystallite size measured by X-ray diffraction (data source: Ref. 34).

its modifications, Eqs. (8), (10), and (11). The data and the analysis results are collected in Table 1. It is seen that many and diverse systems obey these equations, with examples including Pt, Pd, Ag, Ni, or Fe supported on silica, alumina, magnesia, mica, or charcoal, on which H_2 , O_2 , or CO were chemisorbed. Obviously, not *all* che-

misorption data obey Eq. (2), but many do so. Judged from all cases we reanalyzed, about 75% of the chemisorption data can be characterized by a D_c value. Figures 1–3 illustrate some of the cases: A “standard” case of $D_c = 2.0$ ($O_2/Ag/Al_2O_3$ (34), Fig. 1); a common case of $D_c \neq 2$ but close to it ($H_2-O_2/Pt/Al_2O_3$ (24), Fig. 2); and a rare

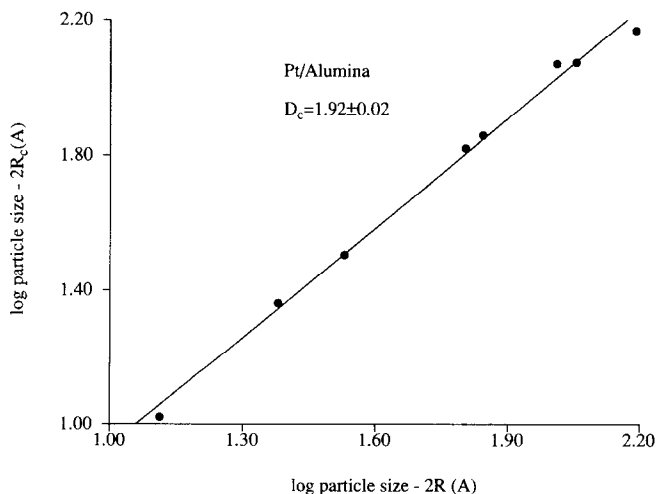


FIG. 2. Pt crystallite size, $2R_c$ (Å), measured by H_2-O_2 titration as a function of Pt crystallite size measured by microscopy (data source: Ref. 24).

TABLE 1
 D_c from Chemisorptions on Dispersed Metal Catalysts

	Catalyst	Adsorbate	D_c	Particle size (\AA) ^a (no. of points)	Data source ref.
1	Rh/Al ₂ O ₃	H ₂ , O ₂ , H ₂ -O ₂ tit.	2.00 ± 0.03	10-150' (4)	19
2	Rh/Al ₂ O ₃	O ₂	1.87 ± 0.09	10-54' (10)	20b
3	Rh/Al ₂ O ₃	H ₂ , H ₂ -O ₂ tit.	1.89 ± 0.07	17-150' (4)	21
4	Rh/Al ₂ O ₃	H ₂ , O ₂ , H ₂ -O ₂ tit.	1.93 ± 0.07	17-150' (4)	22
5	Rh/Al ₂ O ₃	H ₂ , O ₂	2.30 ± 0.05	10-100' (4)	4a ^b
6	Pt/SiO ₂	H ₂	1.81 ± 0.01	30-100' (3)	23
7	Pt/SiO ₂	H ₂	1.95 ± 0.11	30-100'' (4)	23
8	Pt/SiO ₂	H ₂	1.67 ± 0.05	13-40' (5)	2 ^b
9	Pt/Al ₂ O ₃	H ₂ -O ₂ tit.	1.92 ± 0.02	10-120' (11)	24
10	Pt/Al ₂ O ₃	H ₂ -O ₂ tit.	2.09 ± 0.14	15-39' (7)	20a
11	Pt/Al ₂ O ₃	CO	1.95 ± 0.20	13-46'' (4)	25
12	Pt/Al ₂ O ₃	H ₂	1.96 ± 0.11	13-46'' (7)	25
13	Pt/ Ω zeolite	H ₂	1.98 ± 0.03	10-52'' (11)	26
14	Pt/C electrocatalyst	H ₂ , O ₂ ,	2.10 ± 0.23	c'' (16)	27
15	Pt/C electrocatalyst	H ₂	1.87 ± 0.15	28-90 ^d (10)	28
16	Pd/SiO ₂	H ₂	1.94 ± 0.24	80-160'' (5)	29
17	Pd/SiO ₂	CO	2.05 ± 0.23	80-160'' (4)	29
18	Pd/SiO ₂	CO	1.98 ± 0.11	20-140' (7)	30
19	Pd/mica	CO	2.03 ± 0.04	18-74' (8)	31
20	Ag/SiO ₂	O ₂	1.98 ± 0.03	30-500' (7)	32
21	Ag/SiO ₂	O ₂	2.04 ± 0.04	30-500'' (7)	32
22	Ag/SiO ₂	O ₂	2.09 ± 0.04	30-500' (5)	32
23	Ag/SiO ₂	O ₂	1.99 ± 0.17	30-500'' (5)	32
24	Ag/SiO ₂	O ₂	2.05 ± 0.05	50-450' (8)	33
25	Ag/Al ₂ O ₃	O ₂	2.02 ± 0.05	300-730'' (11)	34
26	Ni/Al ₂ O ₃	H ₂	2.34 ± 0.13	40-100' (4)	35

TABLE 1—Continued

	Catalyst	Adsorbate	D_c	Particle size (\AA) ^a (no. of points)	Data source ref.
27	Ni/Al ₂ O ₃	H ₂	2.16 ± 0.06	70–110 ^I (3)	36
28	Ni/SiO ₂	H ₂	2.13 ± 0.12	30–215 ^I (9)	35
29	Ni/SiO ₂	CO	2.06 ± 0.08	25–95 ^{III} (6)	37
30	Ni/SiO ₂	H ₂	1.38 ± 0.04	13–70 ^{III} (24)	38
31	Ni/SiO ₂	H ₂	2.05	e ^{III} (25)	39
32	Ni/SiO ₂	H ₂	1.96 ± 0.20	33–77 ^{II} (12)	40
33	Fe/C	CO	1.57 ± 0.08	13–57 ^{I,II} (7)	41
34	Fe/MgO	CO	1.89 ± 0.09	70–420 ^{II} (3)	42
35	Cu/ZnO	O ₂	2.09 ± 0.10	55–920 ^{II} (6)	43

^a Particle size determined from *I*—microscopy; *II*—X-ray; *III*—magnetism.

^b D_c calculated in that reference.

^c The particle size is given in the paper in terms of the area calculated from it, $A_{x\text{-ray}}$. From Eq. (8), $A_{av} = kA_{x\text{-ray}}^{3-D_c}$.

^d The method for particle size determination is not specified in that reference.

^e D_c was calculated directly from the magnetization value, α , ($\alpha \propto (2R)^3$).

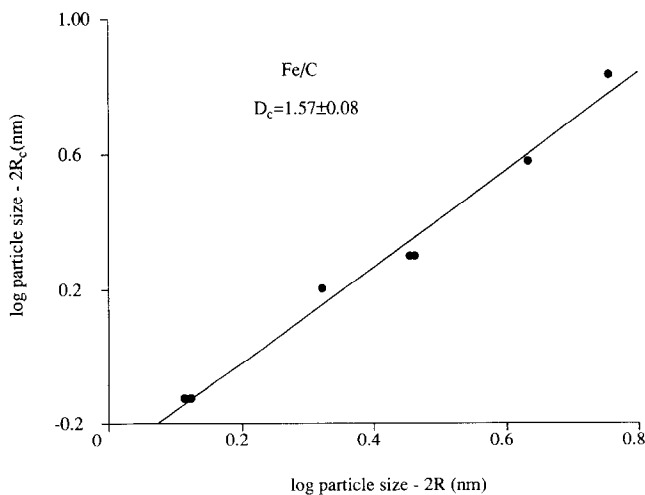


FIG. 3. Fe crystallite size, $2R_c$ (\AA), measured by CO chemisorption as a function of Fe crystallite size measured by X-ray diffraction and/or microscopy (data source: Ref. 41).

case of D_c significantly different from 2 (CO/Fe/C (41), Fig. 3). All three were analyzed by Eq. (10).

4. THE ORIGIN OF $D_c \neq 2$ SITUATIONS IN CHEMISORPTION

4.1. Simple Size–Area Relations

As mentioned in the Introduction, we shall seek the most elementary causes for the observation that experiments in chemisorption are described more generally by Eq. (2) than by Eq. (1), and we start by showing that $D_c \neq 2$ situations are revealed even from simple size–area relations.

The counting procedures employed (here and in the other cases below) for populations of various types of surface atoms in various crystal sizes and shapes are those of Van Hardeveld and Hartog (VH) (14). The details of the calculations are given for the first example; all other calculations were performed similarly. The relevant equations are found in VH.

We determined the relation between the number of total surface atoms, N_s , for a size range of $10 < 2R < 100 \text{ \AA}$, a typical range of sizes in most of the experimental studies collected in Table 1. The calculation is demonstrated for an fcc octahedron. The total number of the atoms in the crystallite, N_T , is given by (14)

$$N_T = \frac{1}{3}m(2m^2 + 1), \quad (13)$$

where m is the number of atoms lying on an

TABLE 2

The Total Number of Atoms and the Number of Surface Atoms of fcc Octahedron Crystallites

m	N_T	$2R(\text{\AA})$	N_s
5	85	13	66
10	670	26	326
15	2255	39	786
20	5340	52	1446
25	10424	65	2306
35	28592	91	4626
40	42676	104	6086

TABLE 3

D_c Values for Various fcc Crystallites in the Range $2R \cong 10\text{--}100 \text{ \AA}$

Crystallite type	D_c^a	D_c^b
Octahedron	2.17 ± 0.02	1.99 ± 0.05
	2.02 ± 0.01^c	1.99 ± 0.01^c
Octahedron-max- B_5	2.12 ± 0.02	1.79 ± 0.01
Cubooctahedron	2.01 ± 0.01^c	1.91 ± 0.01^c
	2.20 ± 0.03	1.85 ± 0.02
	2.22 ± 0.12^d	
Cubooctahedron-max- B_5	2.17 ± 0.05	1.72 ± 0.01
Cube	2.17 ± 0.03	1.99 ± 0.01
Cube-max- B_5	2.12 ± 0.01	1.75 ± 0.01

^a D_c was calculated from the relation $N_s \propto (2R)^{D_c}$.

^b Calculated from $N_H = N_p + 2N_c + 3N_e \propto (2R)^{D_c}$.

^c D_c was calculated in the range $2R \cong 100\text{--}1000 \text{ \AA}$.

^d From Ref. (4a).

equivalent edge of the crystallite (14). The size, $2R$, is calculated from $N_T^{1/3}$ as

$$2R = 1.1 \cdot 2.7 \cdot N_T^{1/3}, \quad (14)$$

where 1.1 is an averaged constant for fcc, hcp, and bcc lattice types (14) and 2.7 \AA is taken as an average diameter of a typical metal atom used in catalysis, i.e., of those collected in Table 1. The resulting $2R$ values are indicated in Table 2. The total number of surface atoms, N_s , calculated from (14)

$$N_s = 4m^2 - 8m + 6 (= n_p), \quad (15)$$

are also collected in Table 2.

The data in Table 2 obey Eq. (2) (Fig. 4) with $D_c = 2.17 \pm 0.02$ (corr. coeff. 0.999). Similar calculations were carried out for various common crystallite shapes. The results are collected in Table 3. It is seen that in all cases $D_c \geq 2.0$. The origin of this phenomenon is in the small size of the objects involved ($10\text{--}100 \text{ \AA}$) compared to the size of the building block ($\sim 3 \text{ \AA}$). In general, for spheroidal objects,

$$N_s^{1/2} \propto N_T^{1/3}. \quad (16)$$

This, however, is not the case for the *small*

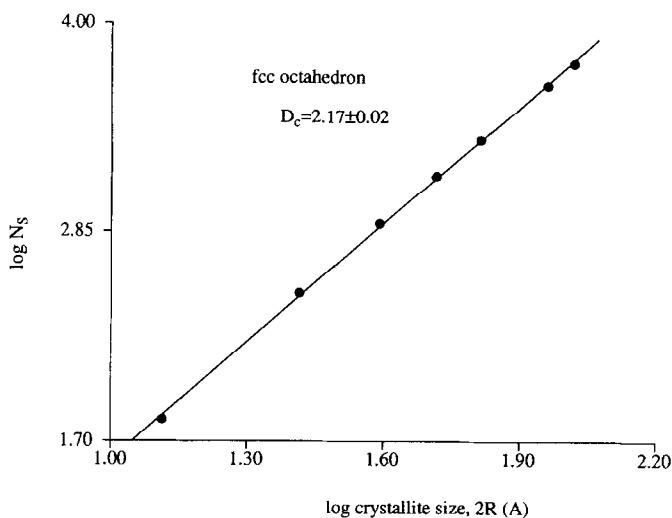


FIG. 4. The number of surface atoms, N_S (or chemisorption sites, n_p , for 1:1 stoichiometry), of an fcc octahedron as a function of its size, $2R$.

crystallites: In small assembled objects with a low ratio between the total size and the building block size, the ratio between N_S and N_T is much higher than the one given by Eq. (16). Recall that, for an assembly of only few spheres, $N_S = N_T$, i.e., Eq. (16) will appear as $N_S^{1/3} \propto N_T^{1/3}$ (an apparent $D_c = 3$). In sufficiently large crystallites, the N_T/N_S ratio approaches the one given by Eq. (16), as is indeed shown for the octahedron: When the $2R$ range is shifted one order of magnitude larger (100–1000 Å, Table 3) the D_c value drops to 2.02 ± 0.01 . We conclude that although the apparent D_c value gradually increases as the crystallite size decreases, in the range of sizes which parallels many experimental studies a single $D_c > 2$ still characterizes very well the N_S/N_T ratio. The theoretically expected very slight concavity of the curves which indeed can be detected in Fig. 4 is probably smeared out by the normal error bars in the case of experiments.

4.2 The Effects of the Chemisorption Stoichiometry

Calculations of surface area and particle size from the chemisorption capacity of gases are usually based on the assumption

of 1:1 stoichiometry (1 adsorbed species:1 surface atom), as employed in the previous Section. This means that the overall chemisorption stoichiometry of a particle is independent of its size. Often, however, this is not the case: Many investigators recognized that chemisorption stoichiometry may change with size (15). For example, Bond suggested that edge and corner atoms are able to adsorb more than one H atom (15a), so that the chemisorption capacity is given by

$$N_H = N_p + 2N_e + 3N_c \quad (= n_p), \quad (17)$$

where N_H is the total number of the adsorbed species (H or other) and the indices, p, e, c indicate plane, edge, or corner atoms, respectively. See Ref. (15) for further discussion of this phenomenon.

Our aim has been to find out whether non-unity stoichiometries are still describable by Eq. (2) Figure 5 demonstrates that Eq. (2) is indeed applicable for these cases as well: Chemisorption on an fcc cubooctahedron with the stoichiometry of Eq. (17) yields $D_c = 1.85 \pm 0.02$. D_c values for other crystallites employing the same stoichiometry are collected in Table 3. It is seen that the resulting D_c values are smaller than the

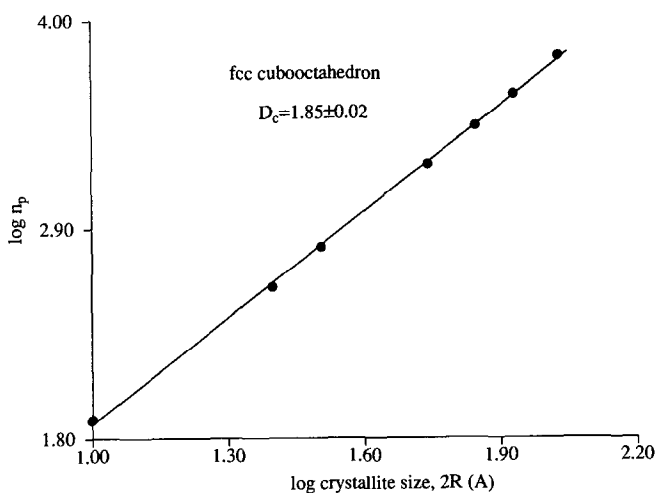


FIG. 5. The number of chemisorption sites, n_p , on an fcc cubooctahedron surface as a function of its size, $2R$. n_p was calculated by assuming the stoichiometry of Eq. (17).

D_c values found in Section 4.1 and even smaller than 2. Obviously, the source for $D_c > 2$ values in the case of 1:1 stoichiometry is shadowed by an even stronger effect. To understand the origin of the decrease in the D_c values, we first recall (14, 16) that if 1:1 chemisorption occurs exclusively on the edges of a crystal, then $N_e \propto (2R)^1$ (actually D_c is slightly larger than 1) (5), and similarly $N_c \propto (2R)^0 = \text{const.}$ for chemisorption on corners. Therefore, by employing the stoichiometry of Eq. (17), one artificially increases the relative contribution of this type of surface-site population. It is as if one has a particle of size $2R$, but with double the normal length of edges (and triple the number of corners). One thus increases the weight of sites which tend to decrease D_c . Indeed, for max-B₅ crystallites, which contain a relatively high proportion of edges (14), the decrease in D_c is especially evident (Table 3). Similarly, D_c increases with size very slowly for the max-B₅ crystallites, as is evident, for instance, for fcc octahedron max-B₅ in the 100–1000 Å range ($D_c = 1.91 \pm 0.01$, Table 3). Interestingly, for the octahedron and the cube, the two opposing effects cancel each other, and one obtains the “classical” $n_p \propto (2R)^2$ situation.

Finally, note that if the stoichiometry is

different from 1:1 but still constant for all particle sizes (say, only 50% of the surface sites are occupied and the rest are a constant percentage of poisoned sites), then D_c will be the same as calculated in Section 4.1. The specific non-1:1 stoichiometry will show up in the prefactor of Eq. (2).

4.3. The Effect of Changes in the Relative Proportion of Crystallographic Planes

Whereas in the previous two sections we dealt with ideal crystallites, here we introduce nonideality in the form of changing proportions of the types of crystal planes (17) as a function of particle size, again, for typical experimental crystallite size range of 10–100 Å. We vary the proportions of the {100}, {110}, and {111} planes and assume that they change gradually with size.

As an example we follow the details of the calculation of D_c for an fcc crystallite composed of {111} and {110} planes; these are collected in Table 4. We follow the first line in the columns of Table 4 from left to right. For a spherical particle of size $2R = 10$ Å, the area, A_p (sphere), is calculated (1257 Å²). We assume that a certain percentage of the surface (20%; 251 Å²) is occupied by {111} planes, and convert it to the number of chemisorption sites (251 Å²/

TABLE 4

The Calculation of the Total Number of Chemisorption Sites of an fcc Crystallite Composed of (111) and {110} Planes

$2R$ (Å)	A_p (Å ²)	(111) Planes (%)	Area of (111) planes (Å ²)	No. of chemisorption sites on (111) planes	Area of {110} planes (Å ²)	No. of chemisorption sites on {110} planes	Total no. of chemisorption sites
10	1,257	20	251	314	1,006	774	1,088
20	5,027	30	1,508	1,885	3,519	2,707	4,592
30	11,310	35	3,959	4,949	7,351	5,655	10,604
40	20,106	40	8,042	10,053	12,064	9,280	19,333
50	31,416	50	15,708	19,635	15,708	12,083	31,718
60	45,239	55	24,881	31,101	20,358	15,660	46,761
70	61,575	60	36,945	46,181	24,630	18,946	65,127
80	80,425	70	56,298	70,373	24,127	18,559	88,932
90	101,788	75	76,341	95,426	25,447	19,575	115,001
100	125,664	80	100,531	125,664	25,133	19,333	146,997

^b The other plane type is {110} for the first four entries, and {100} for the last three.

0.80 Å² = 314). The factor 0.80 Å² is the area, s , available for 1:1 chemisorption stoichiometry of a primitive unit cell of an fcc crystallite, for the (111) plane. The primitive unit cells were calculated according to (18).

$$s = \frac{1}{4} \cdot Q \cdot r_a^2 (h^2 + k^2 + l^2)^{1/2} \quad (\text{fcc}) \quad (18a)$$

$$s = \frac{1}{2} \cdot Q \cdot r_a^2 (h^2 + k^2 + l^2)^{1/2} \quad (\text{bcc}), \quad (18b)$$

where h, k, l are the Miller indices; Q is a constant equal to 1 for structures based on an fcc lattice when h, k, l are all odd, and for the bcc structure when $h + k + l$ is even; $Q = 2$ otherwise, and r_a is the atom size radius (18) (an average value of 1.36 Å was taken). Similarly obtained is the s value for the {110} plane, 1.30 Å². We continue to follow the first line in Table 4: The rest of the surface (80%; 1006 Å²) is composed of {110} planes, which contain 1006 Å²/1.30 Å² = 774 chemisorption sites. So for the crystallite of size $2R = 10$ Å we have a total n_p of 1088 sites, and so on. D_c is then calculated from Eq. (2). The result (Fig. 6) of $D_c > 2$ ($D_c = 2.13 \pm 0.01$) is consistent with gradual increase in the percentage of the more closed plane with particle size, leading to a growth rate in the number of chemisorption

sites, which is faster than $D_c = 2$. And indeed, if the trend is reversed, i.e., if the relative amount of {110} grows with particle size (Table 5), $D_c < 2$ ($D_c = 1.88 \pm 0.02$, Fig. 7) is obtained, reflecting the smaller density of sites on that plane. As a blank calculation we determined that if the ratio between the areas occupied by the two types of planes does not change with size (shown for a fixed (30)% of (111) in Table 5), then the overall density of sites is constant, and $D_c = 2$ should be obtained, as is indeed the case ($D_c = 2.000 \pm 0.001$).

Similar calculations (Table 5) were performed on bcc ((111), $s = 3.20$ Å²; {110}, $s = 1.30$ Å²) and the rationalization of the resulting D_c values is along similar lines: A gradual increase of the relative amount of the more open plane with size, results in a low D_c value, and vice versa: An increasing contribution from the closed plane with size causes $D_c > 2$. For the case of fcc with (111) and {100} ($s = 0.92$ Å²) D_c is virtually 2.0 (Table 5) as a result of the closeness of the corresponding s values.

5. Some Additional Comments

(a) The relation between Eq. (10) and Eq. (12). As mentioned in Section 2, the above equations are seemingly contradictory. In-

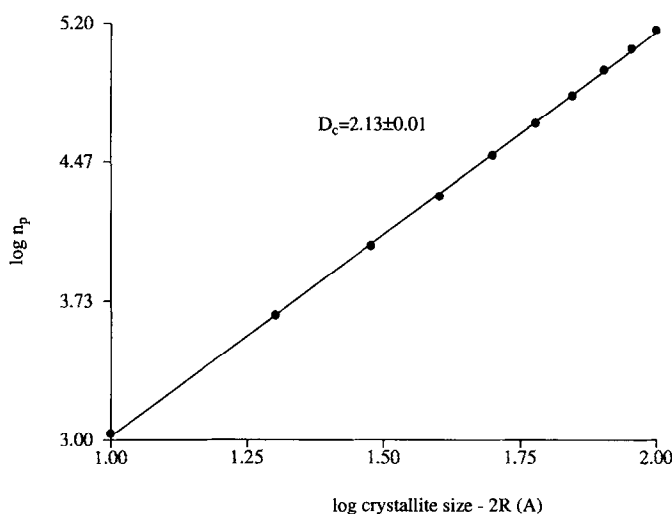


FIG. 6. The number of chemisorption sites, n_p , on an fcc crystallite composed of (111) and {110} planes, as a function of its size, $2R$. The relative proportion of the (111) planes was increased (from 20 to 80%) while that of the {110} planes decreased (from 80 to 20%), with increasing crystallite size.

deed, the deviation of the R_c value from the real R value depends on how R_c is calculated. Based on single particle considerations, Eq. (12) is obtained. But in the transition to per g units, an additional erroneous assumption is made, namely, that a g of the metal contains kR_c^{-3} particles (instead of kR^{-3}). Thus, to retrieve Eq. (10) from Eq. (12), one has to introduce this additional error. To do so, we first bring Eq.

(12) to the form of area units (as is Eq. (10)), $R_c^2 = kR^{D_c}$, and then multiply it by the erroneous assumption $R_c^{-3} = R^{-3}$.

(b) *Estimation of the error made by the use of the assumption in Eq. (1).* Figure 8 demonstrates what could be typical errors in estimating $2R$ if the basic assumption of Eq. (1) is made. We do so by plotting Eq. (8) for D_c values of 1.8, 2.0, and 2.2. It is seen, for instance, that if the measured sur-

TABLE 5

D_c Values for Crystallites with Size-Dependent Ratio of Crystallographic Planes

Lattice type	The change in percentage of various planes with increase in crystallite size ^a			D_c
	(111) ^b , %	{110}/(111), %	{100}/(111), %	
fcc	20 → 80	80 → 20		2.13 ± 0.01
fcc	80 → 20	20 → 80		1.88 ± 0.02
bcc	20 → 80	80 → 20		1.78 ± 0.03
bcc	80 → 20	20 → 80		2.23 ± 0.02
fcc	20 → 80		80 → 20	2.037 ± 0.004
fcc	80 → 20		20 → 80	1.964 ± 0.005
fcc	const. (30)		const. (30)	2.000 ± 0.001

^a Arrows indicate a gradual increase of $2R$ from 10 to 100 Å as demonstrated in Table 4.

^b The other plane type is {110} for the first four entries, and {100} for the last three.

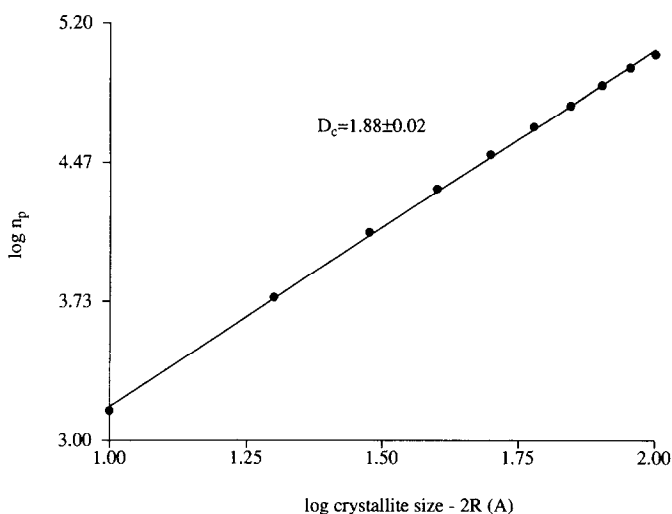


FIG. 7. As in Fig. 6, but with decreasing proportion of the (111) planes (from 80 to 20%) and increasing proportion of the {110} planes (from 20 to 80%) with increasing crystallite size.

face area is $100 \text{ m}^2/\text{g}$, then assuming $D_c = 2$ for materials which have actually a D_c value of 2.2 leads to an underestimation of $2R$ by a factor of ~ 2 , and to an overestimation by a similar factor if the actual D_c value is 1.8.

(c) *The Very Low D_c Values.* In the above sections we have shown two main points: First, that most D_c values fall in the range 1.8–2.2, and second, that simple surface

counting procedures are sufficient to account for this observation. Two exceptions in Table 1 (entries 30, 33) serve to draw attention to the fact that D_c values outside the above range, although rare, may exist and need interpretations beyond those presented above. In the particular case of $D_c = 1.38 \pm 0.04$ for H_2 chemisorption on Ni/SiO₂ (entry 30) (38), the authors, who noted

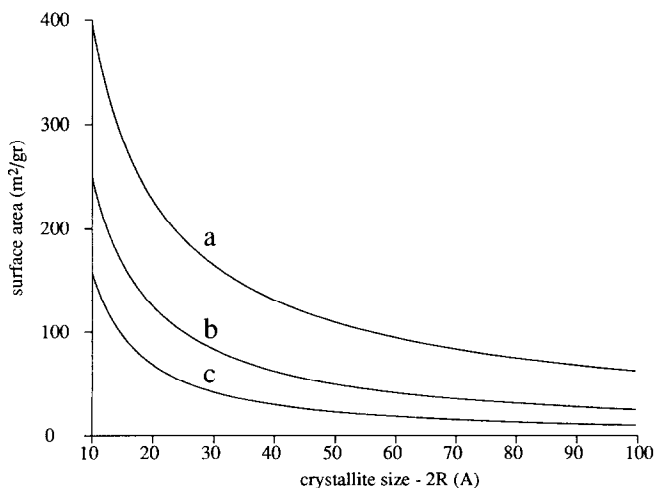


FIG. 8. Surface area A (m^2/gr) as a function of crystallite size, $2R$. A was calculated from the relation $A = k(2R)^{D_c-3}$ for (a) $D_c = 2.2$; (b) $D_c = 2.0$; (c) $D_c = 1.8$ ($k \sim 2500 \text{ \AA}^3/\text{g}$ for a typical metal atom used in catalysis, e.g., Pt).

the weak dependence on Ni particle size (as determined from magnetic measurements), suggest that the crystallites are partially buried and trapped in the pores of the silica, and that the degree of burial (given as an accessibility factor) decreases significantly with size, a behavior which should, indeed, lead to a low D_c value. This was calculated in this case from (Eqs. (5), (8)) to be

$$\frac{A}{A_{\text{magnet.}}} \propto \frac{A}{R^{-1}} = kR^{D_c-2}. \quad (19)$$

In the case of CO/Fe/C (entry 33) (41), for which $D_c = 1.57 \pm 0.08$ was obtained (Fig. 3), a claim is made (41a) that the study confirmed a good agreement between $2R_c$ from chemisorption and $2R$ from microscopy and X-ray diffraction. The analysis according to Eq. (10) can serve to test such claims. In view of the very low D_c value, it seems to us that it perhaps needs re-evaluation.

ACKNOWLEDGMENTS

Discussions with M. Asscher were of great help. This research was supported by the Belfer Foundation and by the Bergmann Foundation. D.F. thanks the Pikovski Foundation and the Aronberg Foundation for support.

REFERENCES

1. Ng, S. H., Fairbridge, C., and Kaye, B. H., *Langmuir* **3**, 340 (1987).
2. Pfeifer, P., *Chimia* **39**, 120 (1985).
3. Avnir, D., Farin, D., and Pfeifer, P., *J. Colloid Interface Sci.* **103**, 112 (1985).
4. (a) Perez, O. L., Romeu, D., Gomez, A., and Yacaman, M. J., "Extended Abstracts of the MRS Meeting 'Fractal Aspects of Materials II'" (D. W. Schefer, R. R. Leibivitz, B. B. Mandelbrot, and S. H. Liu, Eds.), 1986. cf. also (b) Perez, O. L., Romeu, D., and Yacaman, M. J., *J. Catal.* **79**, 240 (1983); (c) Romeu, D., Gomez, A., Perez-Ramirez, J. G., Silva, R., Perez, O. L., Gonzalez, A. E., and Yacaman, M. J., *Phys. Rev. Lett.* **57**, 2552 (1986).
5. (a) Farin, D., and Avnir, D., *J. Amer. Chem. Soc.* **110**, 2039 (1988); (b) Farin, D., and Avnir, D., in "Proceedings, 9th Congr. Catal." (M. J. Phillips, and M. Ternan, Eds.), Vol. 3, pp. 998-1005. Chem. Inst. Ottawa, 1988.
6. (a) Carberry, J. J., *J. Catal.* **107**, 248 (1987); (b) Carberry, J. J., *J. Catal.* **114**, 277 (1988).
7. Fung, D. P. C., Fairbridge, C., and Anderson, R., *Fuel* **67**, 753 (1988).
8. Farin, D., and Avnir, D., *J. Phys. Chem.* **91**, 5517 (1987).
9. Avnir, D., Ed., "The Fractal Approach to Heterogeneous Chemistry." Wiley, Chichester, 1989.
10. Anderson, J. R., "Structure of Metallic Catalysts." Academic Press, New York/London, 1975.
11. Boudart, M., and Djega-Mariadassou, G., "Kinetics of Heterogeneous Catalytic Reactions." Princeton Univ. Press, Princeton, NJ, 1984.
12. Kral, H., *Chem. Eng. Technol.* **11**, 228 (1988).
13. (a) Van-Damme, H., Levitz, P., Gatineau, L., Alcover, J. F., and Fripiat, J. J., *J. Colloid Interface Sci.* **122**, 1 (1988); (b) Ben-Ohoud, M., Obrecht, F., Gatineau, L., Levitz, P., and VanDamme, H., *J. Colloid Interface Sci.* **124**, 156 (1988).
14. (a) Van Hardeveld, R., and Hartog, F., *Surf. Sci.* **4**, 396 (1966); (b) Van Hardeveld R., and Hartog, F., *Surf. Sci.* **15**, 189 (1969).
15. (a) Bond, G. C., "Proceedings, 4th Int. Congr. Catal." 266, Paper #67 (1968); (b) Wilson, G. R., and Hall, W. K., *J. Catal.* **17**, 190 (1970); (c) Karnaukhov, A. P., *Kinet. Katal.* **12**, 1345 (1971); (d) Ladas, S., Poppa, H., and Boudart, M., *Surf. Sci.* **102**, 151 (1981); (e) Ladas, S., *Surf. Sci.* **175**, L681 (1986); (f) Kip, B. J., Duivenvoorden, F. B. M., Koningsberger, D. C., and Prins, R., *J. Catal.* **105**, 26 (1987); (g) Wijnen, P. W. J. G., Van Zon, F. B. M., and Koningsberger, D. C., *J. Catal.* **114**, 469 (1988), and references therein.
16. (a) Taylor, H.S., and Cauer, A. W., *J. Amer. Chem. Soc.* **45**, 920 (1923); (b) Armstrong, E. F., and Hilditch, T. P., *Trans. Faraday Soc.* **17**, 669 (1921); (c) Schwab, G. M., and Rudolph, L., *Z. Phys. Chem. B* **12**, 427 (1931).
17. (a) Yacaman, M. J., and Gomez, A., *Appl. Surf. Sci.* **19**, 348 (1984); (b) Marks, L. D., *Surf. Sci.* **150**, 358 (1985).
18. Nicholas, J. F., Ed., "An Atlas of Models of Crystal Surfaces." Gordon & Breach, New York, 1965.
19. Coq, B., and Figueras, F., *J. Molec. Catal.* **40**, 93 (1987).
20. (a) Boitiaux, J. P., Cosyns, J., and Robert, E., *Appl. Catal.* **32**, 145 (1987); (b) Boitiaux, J. P., Cosyns, J., and Robert, E., *Appl. Catal.* **32**, 169 (1987).
21. Del Angel, G., Coq, B., Dutartre, R., and Figueras, F., *J. Catal.* **87**, 27 (1984).
22. Fuentes, S., and Figueras, F., *J. Catal.* **61**, 443 (1980).
23. Sagert, N. H., and Pouteau, R. M. L., *Canad. J. Chem.* **49**, 3411 (1971).
24. Barbier, J., Morales, A., and Maurel, R., *Bull. Soc. Chim. Fr.* **1-2**, 1-31 (1978).

25. Renouprez, A., Hoang-Van, C., and Compagnon, P. A., *J. Catal.* **34**, 411 (1974).
26. Coq, B., Figueras, F., and Rajaofanova, V., *J. Catal.* **114**, 321 (1988).
27. Connolly, J. F., Flannery, R. J., and Aronowitz, G., *J. Electrochem. Soc.* **113**, 577 (1966).
28. Kinoshita, K., and Stonehart, P., *Electrochim. Acta* **20**, 101 (1975).
29. Moss, R. L., Pope, D., Davis, B. J., and Edwards, D. H., *J. Catal.* **58**, 206 (1979).
30. Le-Page, J.-F., *et al.*, Eds. "Applied Heterogeneous Catalysis: Design, Manufacture, Use of Solid Catalysts," p. 212. Editions Technip. Paris, 1987.
31. (a) Doering, D. L., Poppa, H., and Dickinson, J. T., *J. Vac. Sci. Technol.* **18**, 460 (1981); (b) Doering, D. L., Poppa, H., and Dickinson, J. T., *J. Catal.* **73**, 104 (1982).
32. Wu, J. C., and Harriott, P., *J. Catal.* **39**, 395 (1975).
33. Jarjoui, M., Gravelle, P. C., and Teichner, S. J., *J. Chim. Phys.* **75**, 1069 (1978).
34. Verykios, X. E., Stein, F. P., and Coughlin, R. W., *J. Catal.* **66**, 368 (1980).
35. Mustard, D. G., and Bartholomew, C. H., *J. Catal.* **67**, 186 (1981).
36. Fujiyama, T., Otsuka, M., Tsuiki, H., and Ueno, A., *J. Catal.* **104**, 323 (1987).
37. Primet, M., Dalmon, J. A., and Martin, G.A., *J. Catal.* **46**, 25 (1977).
38. Richardson, J. T., and Koveal, R., *J. Catal.* **98**, 559 (1986); cf. also Desai, P., and Richardson, J. T., in "Catalyst Deactivation" B. Dalmon and G. F. Froment, Eds. p. 149. Elsevier, Amsterdam, 1980.
39. Schuit, G. C. A., and Van-Reijen, L. L., in "Advances in Catalysis" (D. D. Eley, H. Pines, and P. B. Weisz, Eds.), Vol. 10, p. 242. Academic Press, New York, 1958.
40. Fu, L., Kung, H. H., and Sachtler, W. M. H., *J. Molec. Catal.* **42**, 29 (1987).
41. (a) Guerrero-Ruiz, A., Rodriguez-Ramos, I., and Romero-Sanchez, V., *React. Kinet. Catal. Lett.* **28**, 419 (1985), (b) Guerrero-Ruiz, A., de Lopez-Gonzalez, J., Mata-Arjona, A., Romero-Sanchez, V., and Rodriguez-Ramos, I., *Adsorpt. Sci. Technol.* **3**, 33 (1986).
42. Boudart, M., Delbouille, A., Dumesic, J. A., Khammouma, S., and Topsøe, H., *J. Catal.* **37**, 486 (1975).
43. Parris, G. E., and Klier, K., *J. Catal.* **97**, 374 (1986).